ELSEVIER

Surface Science 366 (1996) 251–259

surface science

The (1 × 2) and (1 × 4) structure on clean Pt(110) studied by STM, AES and LEED

S. Speller, J. Kuntze, T. Rauch, J. Bömermann, M. Huck, M. Aschoff, W. Heiland *

Universität Osnabrück, FB Physik, D-49069 Osnabrück, Germany

Received 14 December 1995; accepted for publication 9 May 1996

Abstract

By different annealing procedures the (1 × 2) and the (1 × 4) structures on Pt(110) are produced on the clean surface. Both structures are verified by STM and LEED. AES shows very low impurity levels of C, O, S, Si and Ca in both cases. In case of the (1 × 4) structure, Si and/or SiO_x signals are not significantly higher than in case of the (1 × 2) structure. The (1 × 2) structure is combined with a perfect "fish-scale" pattern of the step structure. The (1 × 4) structure is connected with large flat terraces bound by steep ledges of a height of 30–40 Å. The (1 × 4) structure is identified as a paired-row (1 × 2) structure.

Keywords: Auger electron spectroscopy; Low energy electron diffraction (LEED); Low index single crystal surfaces; Platinum; Scanning tunneling microscopy (STM)

1. Introduction

The reconstruction of the Pt(110) surface was found in 1972 [1]. It was the second case of a (1 × 2) reconstruction of an fcc(110) surface after the Au case [2]. Higher-order (1 × *n*) structures with *n* = 3, 5 and 7 were found [3] which are at least partly induced by impurities [4,5]. The (1 × 2) structure was identified as a "missing row" structure [1–5] which was independently corroborated by other studies [6–14]. The (1 × 4) structure was only reported in the RHEED study [5], and the result was interpreted as a "rather slightly modified (1 × 2) structure". A large part of these studies is concerned with the (1 × 2)↔(1 × 1) phase transition which we will not discuss here. A recent review also of the theoretical aspects is by Bernasconi and Tosatti [15]. Of direct concern for the present work are the recent STM results on Pt(110) [16,17], which show the "fish-scale" pattern as the mesoscopic step arrangement of the (1 × 2) structure. Also, (1 × *n*) structures with *n* = 3, 5, 7, 9 are found, very probably induced by impurities such as Ca. The fish-scale pattern is also found on Au(110) by STM [18,19]. The fish-scale pattern is caused by small energy differences of (111) and (331) steps [20,21]. The (*hkl*) directions given here define the orientation of the facets formed by the respective steps. In order to form (111) type steps only, which have a lower energy, the surface avoids (331) steps. The (331) steps would be formed if the surface would create rectangular terraces oriented along the [1$\bar{1}$0] and [001] directions on a (1 × 2) reconstructed surface. Instead of rectangular terraces, elongated rhombus-shaped terraces are

* Corresponding author. Fax: +49 541 9692670; e-mail: wheiland@dosuni1.bitnet

0039-6028/96/$15.00 Copyright © 1996 Elsevier Science B.V. All rights reserved
PII S0039-6028(96)00810-2

found, bordered by short (111)-type steps interrupted by very short steps along [001]. In the present work we describe the preparation of the (1×2) and the (1×4) reconstruction and analyse the respective structures with STM.

2. Experimental

For the experiments we use an experimental set-up equipped with three UHV chambers, i.e. the STM chamber, the analysis chamber and a preparation chamber. The first two chambers can be sealed from the preparation chamber by gate valve. Targets are brought into the preparation chamber via a vacuum lock. For the target transfer a manipulator system is used. From the analysis manipulator, the targets are transported into the STM chamber with a wobble stick. This affords short transfer times from the analysis to the STM and vice versa. The analytical equipment consists of a reverse LEED system, and a RHEED electron gun which is used for RHEED and AES. The electron gun (STAIB) is operated at 5 keV for AES. The AE spectra are measured with a 180° electrostatic analyser. With the analyser, "integral" spectra are recorded which are differentiated numerically for comparison with standard data and results of other authors. Targets are prepared by ion bombardment, annealing and gas exposure. For Pt(110) we used exposure to oxygen, as in previously published work. The sputtering gas is Ar, cleaned by liquid-N freezing before entering the ion source. The ion energy is 500 eV. The angle of incidence is varied between 50° and 60° versus the surface. Initial sputter times at beam currents of several μA amount to several h. STM shows at that stage "etch pits" similar to the features reported by Michely et al. [20]. AES occasionally indicates C as an impurity, which is easily removed by oxygen exposure at temperatures of 600 K at a pressure of 10^{-6} hPa for about 1 h. After atomic resolution is obtained in the STM, short sputtering times (< 1 h) are sufficient to clean the surface again. If the clean surface is annealed at temperatures above the $(1\times2)\leftrightarrow(1\times1)$ transition temperature, i.e. above about 950 K for less then 1 h and cooled down with a moderate rate of 5 K min^{-1}, the (1×2) structure is obtained. Annealing below the transition temperature, i.e. 800 K for about 3 h and a slow cooling at 1 K min^{-1}, produces the (1×4) structure.

3. Results

The results obtained are STM "pictures", LEED patterns and AE spectra. The first set of data represents the well-known Pt(110)(1×2) structure. Fig. 1 is a large-scale (2600 Å × 2600 Å) STM picture showing an essentially defect-free fish-scale pattern. The terrace lengths are of the order of 600 Å, and the widths of the order of 100 Å. Defect-free means that at the respective end-point of any given rhombus-shaped terrace, four terraces always meet. In many cases, very long single-atom grooves or hills are formed in order to meet the requirement of the fish-scale. Features like this have not previously been seen as extensively [16,17]. On Au, for comparison, the fish-scale pattern is less perfect [18,19]. On the Pt surface the single-atom wide features (hills and grooves), extend as far as 200 Å. These fragile-looking features are stable for hours.

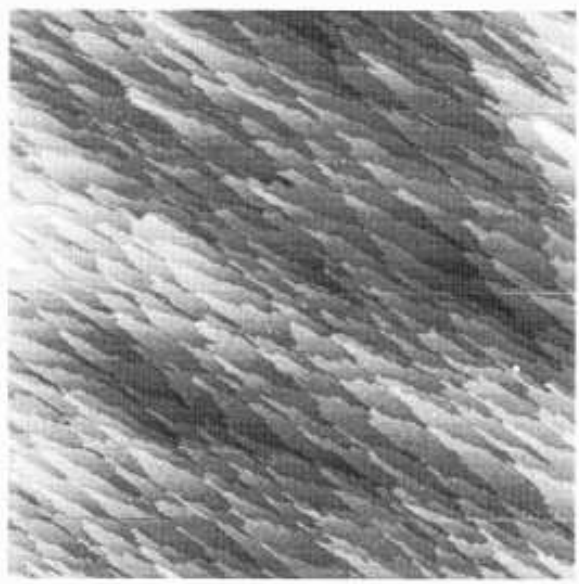

Fig. 1. Large scale (2600 Å × 2600 Å) view of the Pt(110)-(1×2) surface. The [1$\bar{1}$0] surface direction lies about the diagonal in the frame, from the upper left corner to the lower right corner.

We also find cases where two atomic rows form the groove or the hill, with all possible commutations. These details are clearly seen on a smaller scale STM scan (580 Å × 550 Å) (Fig. 2). The AES results for the (1 × 2) structure are shown in Fig. 3. There is weak evidence for some C on the surface, i.e. a small bump in the $N(E)$ spectrum, which disappears in the $dN(E)/dE$ data. Other possible contaminants, e.g. Si, S, Ca and O, are below the detection limit.

The Pt(110)-(1 × 4) structure is shown on a large- scale STM picture in Fig. 4a. There are very large terraces of the order of 1000 Å × 3000 Å with a very regular row structure. The large (1 × 4) plateaus are bordered by steep cliffs, as shown in some detail in Fig. 4b. The average direction of these cliffs is parallel to [111]. The cliffs are too steep, i.e. of a typical height difference of 40 Å over a length of 200 Å, for to be studied in detail by STM. The linescans of Fig. 5 show a distance of the $[1\bar{1}0]$ rows almost equal to that of the (1 × 2) structure, i.e. the (1 × 4) structure is not a missing-row structure. In a small-scale STM scan (Fig. 5a), an alternating depth and/or alternating width feature is seen. The height scan clearly shows alternating depths of the troughs, indicating alternating widths of the troughs. Occasionally a domain boundary of the row-pairing is found, as can be seen in the small scan shown in Fig. 5b (arrow). The existing domains are obviously larger than the transfer length of the LEED-beam. The LEED pattern shows a (1 × 4) reconstruction (Fig. 6).

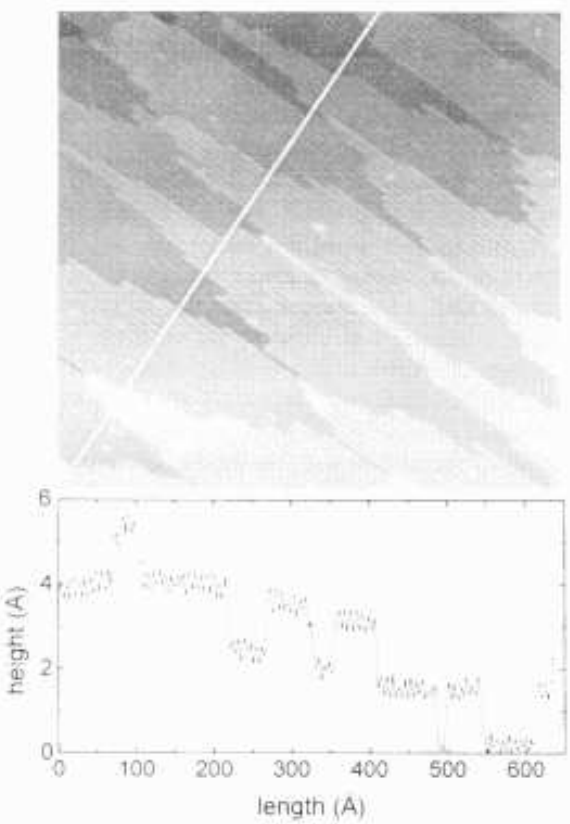

Fig. 2. Close-up (580 Å × 550 Å) of the Pt(110)-(1 × 2) surface. The [110] rows are resolved. The narrowest features are monoatomic rows and valleys. The height scan is parallel to the [001] surface direction.

A Fourier analysis using single linescans of the (1 × 4) structure has peaks at the corresponding lattice constants (Fig. 7). From a numerical simulation of STM-line-scans according to the model shown in Fig. 9 we conclude that the distance between every other pair of top [110] rows is reduced by about 0.3 ± 0.2 Å compared to the (1 × 2) structure, i.e. the (1 × 4) is identified as a pairing-row (1 × 2) structure. The amount of the shift depends linearly on the ratio of the $2a_0$ and $4a_0$ peaks in the Fourier transform of the linescans. If instead of one single linescan a sum of scans, or a sum of Fourier transforms of single scans is taken, we obtain the same result, i.e. the pairing-row structure. From these calculations, we obtain an estimate of the error bar of about ± 0.2 Å. The transform shown in Fig. 7 is that of a sum of linescans, so that noise in the data is averaged out.

The AES results indicate approximately the same amount of impurities as in case of the (1 × 2) structure (Fig. 8). We note, however, that in the integral AE spectrum we see a small peak at the oxygen AE energy. In the differentiated spectrum this small peak is lost in the noise. In order to keep the influence of the electron beam negligible, and to avoid contamination via CO cracking, low electron currents and therefore lower count rates had to be accepted. The intensity of the Pt 237 eV peak in the (1 × 2) spectrum is about 80 000 counts; the same peak in the (1 × 4) spectrum has an intensity of 660 000 counts. Since it is known [21–23] that an Auger O signal may be connected with an Si impurity, there may be a small trace of

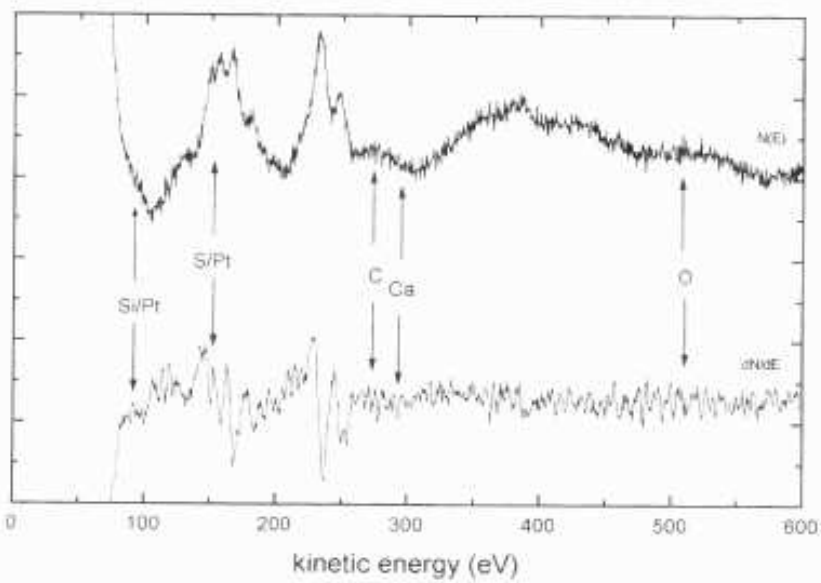

Fig. 3. AES of the clean Pt(110)-(1 × 2) surface. All non-labeled peaks are Pt Auger peaks. Positions of possible impurities are indicated.

Si. After very long heating periods, e.g. 3 h at 1100 K, a clear Si signal representing about 8% Si (peak-to-peak evaluation) is obtained, which can be used for an estimate of the impurity level of the "clean" surface. From this comparison we obtain a level of Si $<1\%$ of a monolayer for the clean case. Comparing our data with the earlier results for Pt(111) [21–23] similar impurity levels are estimated. Regarding this level of "contamination", we conclude that Si has no influence on the (1 × 4) structure. Comparing the (1 × 2) and (1 × 4) spectra, there is no obvious difference with respect to impurities. Hence, the interesting conclusion is that on Pt(110), two "clean" structures can be produced which show a marginal difference in the local structure (pure (1 × 2) versus slightly paired (1 × 2)), but which have a quite different mesoscopic structure (fish-scale versus large flat terraces).

4. Discussion

The Pt(110)-(1 × 2) missing-row structure has been established for many years. It is again confirmed with an impurity level below the detection limits of our system for Si, S, C, Ca and O. The detection limit for Si can be estimated from the spectra with a clear Si signal (Fig. 8). From the usual AES peak-to-peak analysis this Si signal is equivalent to about 8% of a monolayer of Si. That means for "clean" (1 × 2) and (1 × 4), respectively, a Si surface concentration below 1% of a monolayer. In the same spectrum (Fig. 8c) there is also some evidence for S segregation, i.e. an increase of the combined Pt–S peak at 152 eV. This S peak leads to a similar estimate of the S concentration on the clean surfaces of below 1%. Other impurities discussed previously, i.e. C, Ca and O [1,14,21–23], are not detected here above the noise level. So, we conclude that within the detection limits of a reasonable AES system, clean Pt(110) has two surface structure modifications which are identified by LEED and STM. The (1 × 4) structure is in fact a paired-row (1 × 2) structure. The pairing consists of a lateral shift of alternating pairs of the [110] surface chains by less than 0.5 Å (Fig. 9). Pairing has previously been discussed as a possible effect on the (110) surfaces of Au and Pt [24,25] although of a different type to that found here. The energetic differences between pure missing-row structures and paired structures are small, which reflects a general problem of this field, i.e. the energy differences causing reconstructions are always small [15].

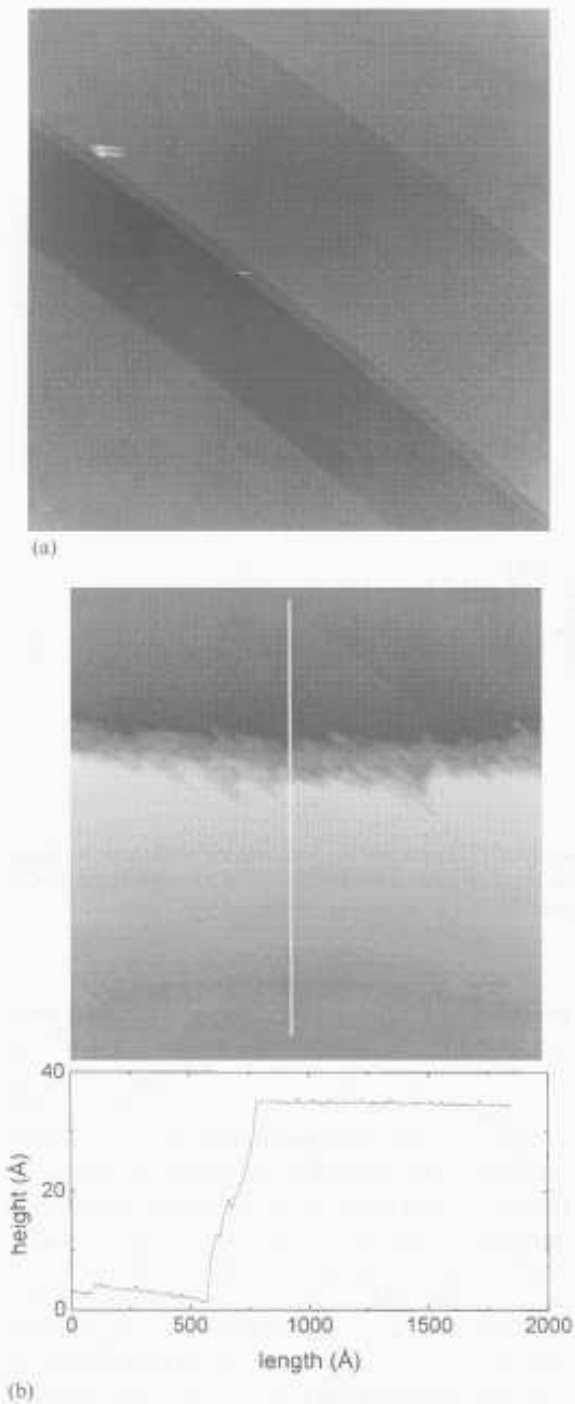

Fig. 4. (a) Large-scale (2600 Å × 2600 Å) view of the Pt(110)-(1 × 4) surface. The [1$\bar{1}$0] rows are not resolved, and lie about diagonal. (b) View of a "cliff" separating two (1 × 4) terraces (2000 Å × 2000 Å). The [1$\bar{1}$0] direction is about the diagonal, from the upper left corner to the lower right corner. The average step direction is [1$\bar{1}$1].

An interesting aspect is the differences of the "mesoscopic" structures, of the (1 × 2) and the (1 × 4) structures respectively. The (1 × 2) structure is combined with a "perfect" fish-scale pattern. In a recent paper [26] the energetics of the fish-scale formation are analyzed. The "driving force" is the energy difference between (111) microfacets with respect to (331) microfacets. It is peculiar to the (1 × 2) structure that rectangular terraces bordered by steps along the [1$\bar{1}$0] and [001] directions are energetically unfavourable because a terrace formed with borders parallel to [1$\bar{1}$0] will inevitably have a (111) facet on one side and a (331) facet on the other side. The (331) facet energy is higher than the (111) facet energy by about 40 meV per atom [15]. In Fig. 10 the "defects" in question are shown. As can be seen in Fig. 10a, when a (1 × 2) terrace is built on a (1 × 2) surface by (i) filling the missing rows and (ii) building the new top (1 × 2) layer, one side of the terrace is a (111) facet or (3 × 1) defect, and the other side is a (331) facet or a (1 × 1) defect. If the terrace is bordered on each side by (111) facets or (3 × 1) defects, the missing-row structures neighbouring the terrace are out of phase by one lattice constant a_0. The step along the [1$\bar{1}$0] direction which forms (111) facets is also called a (3 × 1) step, and the (331) facet is called a (1 × 1) step with energies of 22 and 64 meV per atom, respectively. The possible steps along [001] would have an even higher energy, so that step meandering is "invented" to minimize the free energy. This is the cause for many (3 × 1) steps parallel to the [1$\bar{1}$0] direction connected by monoatomic kinks and/or very short steps in the [001] and [112] directions as seen in Figs. 1 and 2. A further result of the theory is that for the strong chirality regime overhangs are forbidden, and hence step excursions occur in one direction only. Furthermore, steps of the same kind do not cross. For these reasons the rhombic network of steps is formed. The fish-scale pattern has an average slope which may be equal to the macroscopic miscut angle θ. On our Pt(110) surface the average $\theta = 0.3 \pm 0.1°$, which is related to the ratio of the average number of atoms along the [1$\bar{1}$0] and the [001] directions respectively. This ratio is 0.1 in our case. In turn, this ratio can be also expressed by the step-crossing angle ϕ, which in our case is

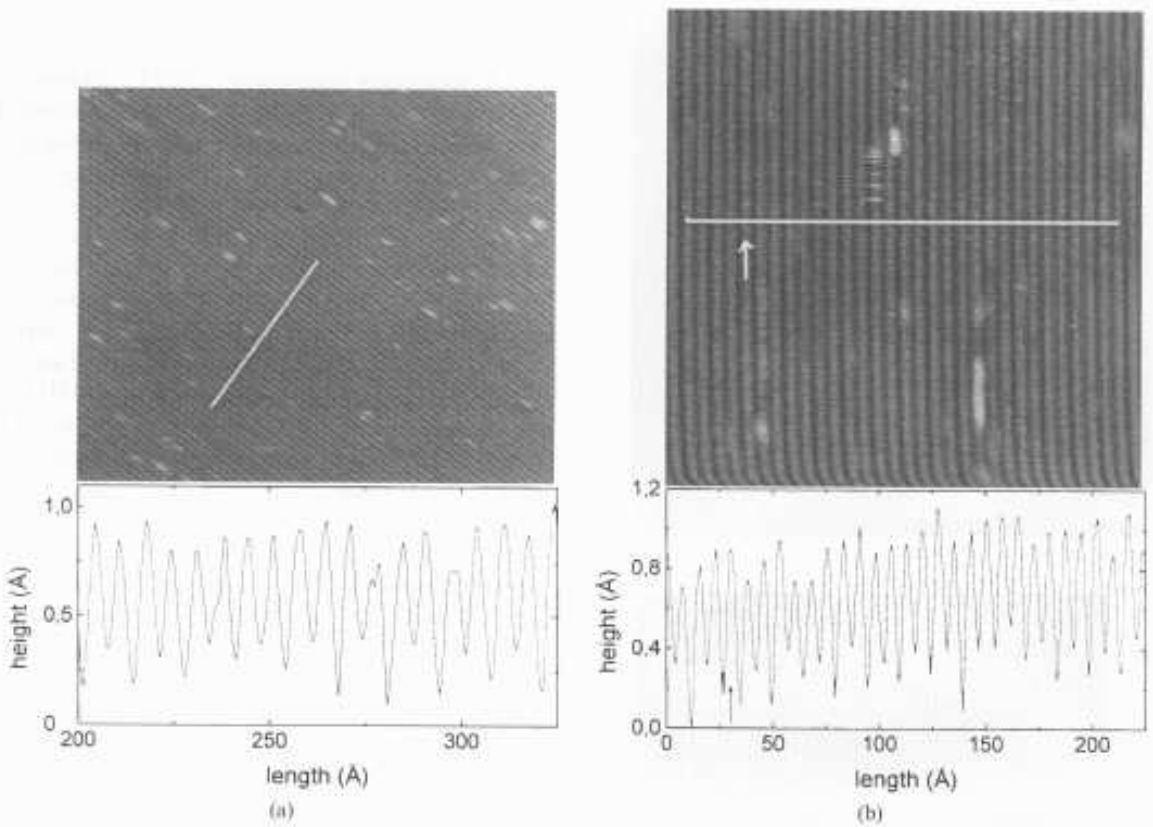

Fig. 5. (a) Small-area view of the Pt(110)-(1 × 4) surface (400 Å × 400 Å). The [1$\bar{1}$0] rows are resolved, and the height scan is parallel to the [001] direction (indicated by the line). (b) Small-area view of the Pt(110)-(1 × 4) surface (250 Å × 250 Å), exhibiting a domain boundary in the row-pairing (marked by the arrow). The boundary is also evident in the linescan along the [001] direction.

$20 \pm 2°$. The step crossing angle ϕ is in case of the limit $\theta \to 0$ related to the energy ϵ per atom of the [1$\bar{1}$0] step sections of the (1 × 3) type via [26]

$$\phi = 2 \tan^{-1}\left[\sqrt{2}\left(e^{\epsilon/k_B T} - 1\right)\right].$$

With our values we obtain $\epsilon \approx 3$ meV per atom. This values agrees with the theoretical value of 2.3 meV estimated on the basis of the critical temperature of Pt(110) [26]. For the (1 × 4) structure we have no basis for a comparable discussion. We note that the experimental average miscut angle $\theta = 0.3°$ for the (1 × 4) is equal to that of the (1 × 2) surface. The pairing found with the STM (Figs. 4 and 5) is different from that discussed previously [24,25]. In Fig. 9 we compare the missing row (1 × 2), the paired-row (1 × 2) and our (1 × 4) structure. Both the AES data and the "defect-free" STM pictures of the (1 × 4) structure suggest that this configuration is another solution for the Pt(110) surface to minimize the energy. In the AE spectra there are no significant amounts of impurities, and even if there is a trace of Si/SiO_x on the (1 × 4) structure, it is not clear how this low concentration may stabilize the structure. Since it is known that in the STM impurities look generally different from the bulk material, we may emphasize that also the STM data suggest that the surface is (at least locally) clean in both cases. There is also no evidence for "step pinning" in the STM data, usually a signature of impurities.

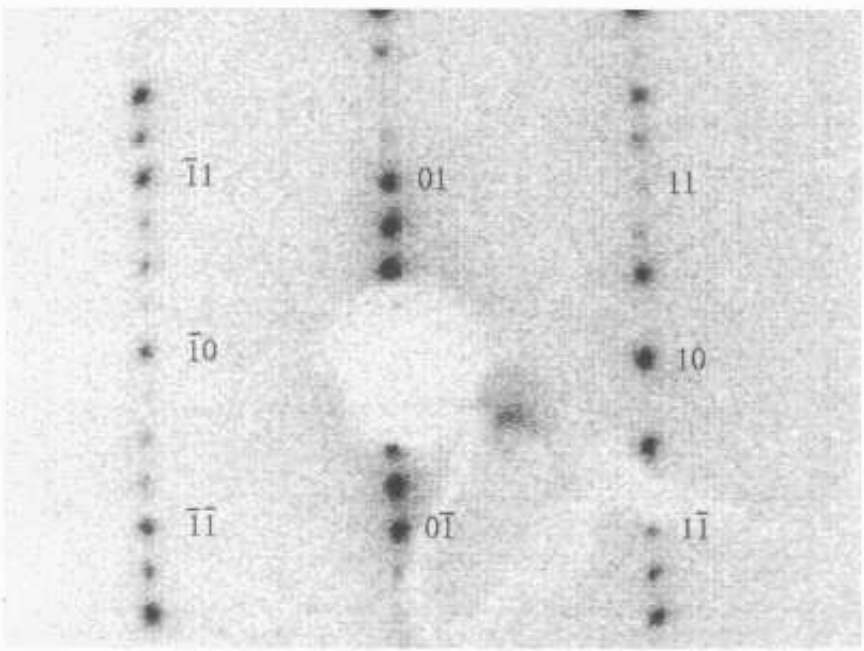

Fig. 6. LEED pattern of the Pt(110)-(1 × 4) surface at 90 eV electron energy.

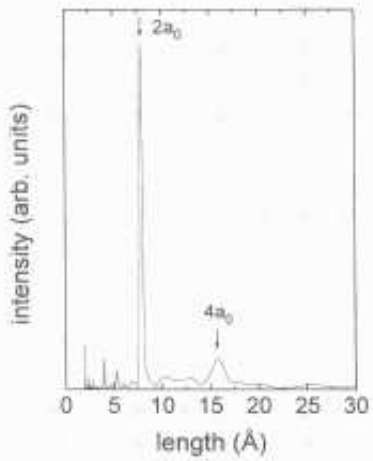

Fig. 7. Fourier analysis results of the (1 × 4) surface. Peaks are found at $2a_0$ and $4a_0$, where a_0 is the regular lattice spacing in the [001] direction.

5. Summary

The known (1 × 2) structure of the Pt(110) surface has been confirmed.

Comparisons of experimental and theoretical results concerning the mesoscopic step structure have been made. We found good agreement and obtain a step energy of 3 meV per atom in the $[1\bar{1}0]$ direction at a (1 × 3) step.

We investigated the (1 × 4) structure of the Pt(110) surface, which was previously reported by Stock et al. but at that time no structural model could be given. The structure has now been identified as a "paired row" structure, i.e. a slightly modified (1 × 2) reconstruction. The distance between every other pair of top $[1\bar{1}0]$ rows is reduced by about 0.3 ± 0.2 Å compared to the ideal missing-row distance of 7.84 Å.

The mesoscopic step structure of the (1 × 4) reconstruction shows very large, flat terraces bordered by steep cliffs. It is therefore totally different to the fish-scale pattern observed for the (1 × 2) structure.

The (1 × 4) structure may be another way for the "clean" Pt(110) surface to minimize its free energy. The influence of traces of possible impurities has to be a matter of further research. In our experiments, no significant amounts of impurities (i.e. higher concentrations than for the (1 × 2) structure) have been found.

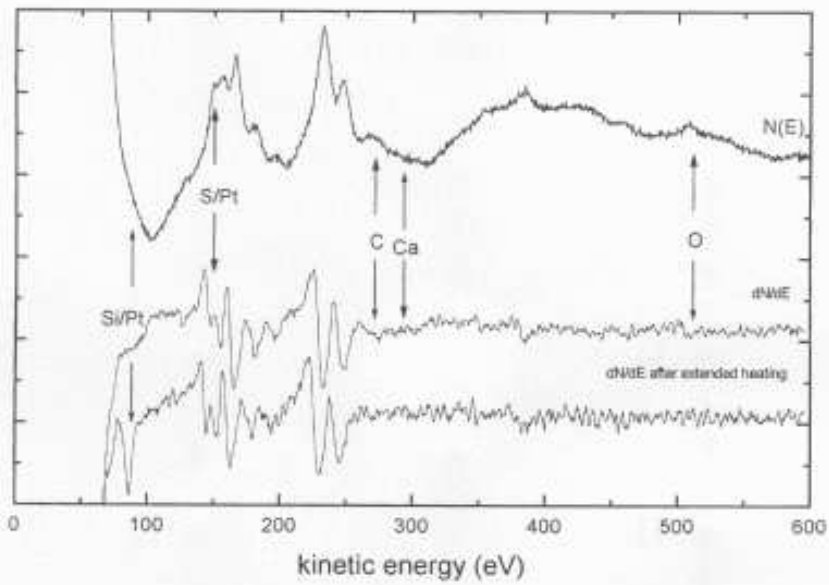

Fig. 8. AES of the Pt(110)-(1×4) surface. Top line: $N(E)$ spectrum of the clean surface. Middle line: differentiated $dN(E)/dE$ spectrum of the top line. Lower line: differentiated spectrum of a Si-contaminated (1×4) surface. All non-labeled peaks are Pt Auger peaks.

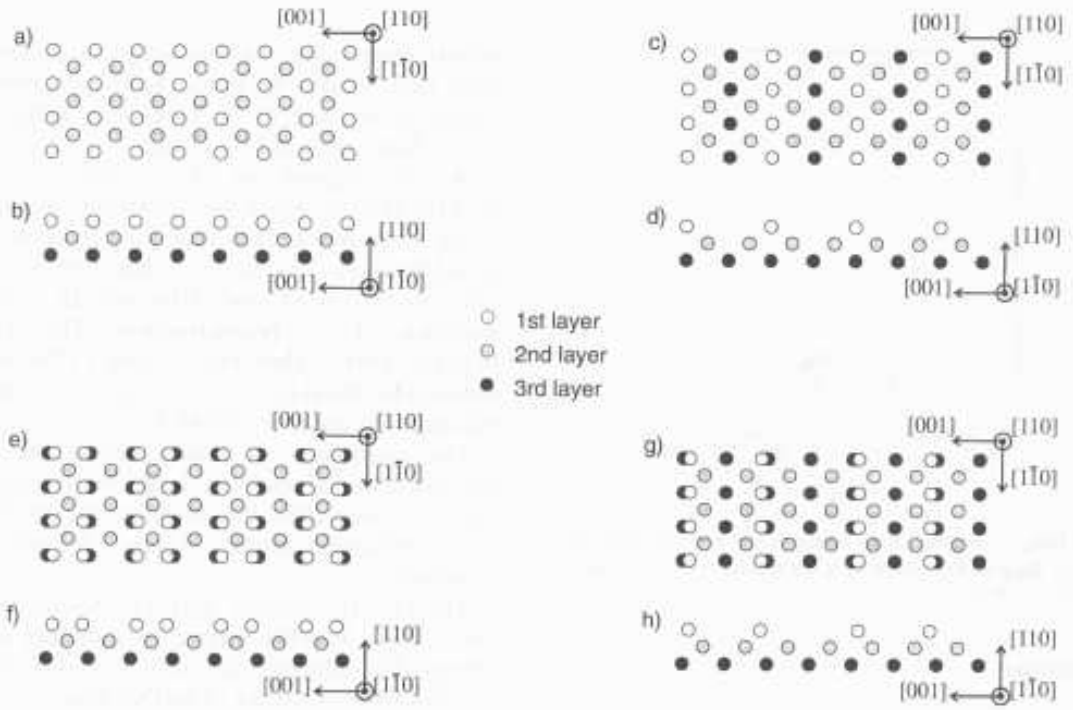

Fig. 9. Models of various structures. (1×1) Structure: (a) top view, (b) side view. Missing-row (1×2) structure: (c) top view, (d) side view. Paired (1×2) structure: (e) top view, (f) side view. Paired (1×4) Pt(110): (g) top view, (h) side view. The (1×4) structure is in fact a missing-row, paired (1×2) structure (g) and (f).

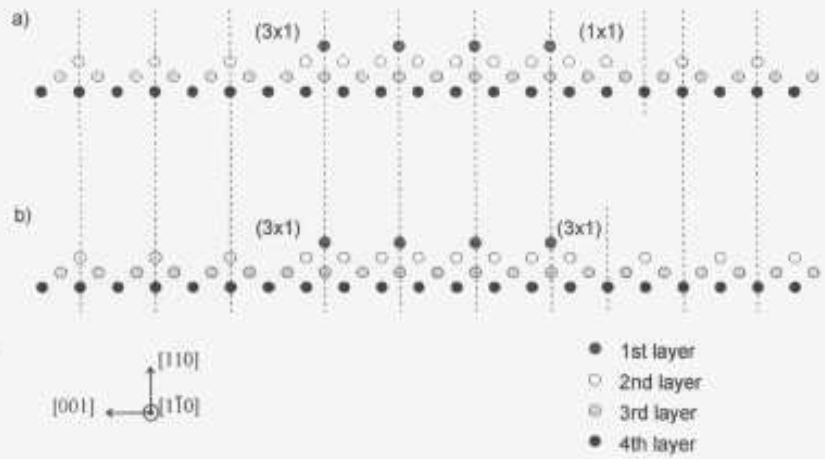

Fig. 10. Models of the defects important for the "fish-scale" formation.

Acknowledgements

This work is supported by the Deutsche Forschungsgemeinschaft (DFG). We thank U. Korte and W. Tappe, Osnabrück, for helpful discussions.

References

[1] H.P. Bonzel and R. Ku, Sci. Technol. 9 (1972) 663.
[2] D.G. Fedak and N.A. Gjostein, Acta Metall. 15 (1967) 827.
[3] M. Salmeron and G.A. Somorjai, Surf. Sci. 91 (1980) 373.
[4] P. Häberle, P. Fenter and T. Gustafsson, Phys. Rev. B 39 (1989); P. Fenter and T. Gustafsson, Phys. Rev. B 38 (1988) 10197.
[5] M. Stock, J. Risse, U. Korte and G. Meyer-Ehmsen, Surf. Sci. 233 (1990) L 243.
[6] H. Niehus, Surf. Sci. 145 (1984) 407.
[7] F. Masson and J.W. Rabalais, Chem. Phys. Lett. 179 (1991) 63.
[8] G.L. Kellog, Phys. Rev. Lett. 55 (1985) 2168.
[9] P. Fery, W. Moritz and D. Wolf, Phys. Rev. B 38 (1988) 7275.
[10] E.C. Sowa, M.A. van Hove and D.L. Adams, Surf. Sci. 199 (1988) 174.
[11] E. Vlieg, I.K. Robinson and K. Kern, Surf. Sci. 223 (1990) 248.
[12] K. Dückers and H.P. Bonzel, Europhys. Lett. 63 (1989) 2578.
[13] S. Holmberg, H.C. Poon and Y. Jugnet, Tran Minh Duc, Surf. Sci. 254 (1991) L 475.
[14] U. Korte and G. Meyer-Ehmsen, Surf. Sci. 298 (1993) 306; Phys. Rev. B 48 (1993) 8345.
[15] M. Bernasconi and E. Tosatti, Surf. Sci. Rep. 17 (1993) 363.
[16] T. Gritsch, D. Coulman, R.J. Behm and G. Ertl, Phys. Rev. Lett. 63 (1989) 1086.
[17] T. Gritsch, D. Coulman, R.J. Behm and G. Ertl, Appl. Phys. A 49 (1989) 403; Surf. Sci. 257 (1991) 297.
[18] J. Gimzewski, R. Berndt and R. Schlittler, Phys. Rev. B 45 (1992) 6844.
[19] S. Speller, T. Rauch and W. Heiland, Surf. Sci. 342 (1995) 224.
[20] T. Michely and G. Comsa, Surf. Sci. 256 (1991) 217.
[21] H. Niehus and G. Comsa, Surf. Sci. 93 (1980) L 147.
[22] H.P. Bonzel, A.M. Franken and G. Pirug, Surf. Sci. 104 (1981) 625.
[23] H. Niehus and G. Comsa, Surf. Sci. 102 (1981) L 14.
[24] J.R. Noonan and H.L. Davis, J. Vac. Sci. Technol. 16 (1979) 587.
[25] M. Manninen, J.K. Nørskov and C. Umrigar, Surf. Sci. 119 (1982) L 393.
[26] I. Vilfan, private communication.